AGU PUBLICATIONS

JGR

Journal of Geophysical Research: Atmospheres

RESEARCH ARTICLE
10.1002/2014JD021567

Key Points:
- IN properties of bare and coated dust particles are investigated
- Aged particles were lacking structured water order that affected IN properties
- Simulated cloud properties were sensitive to the bare and coated particles

Supporting Information:
- Readme
- Table S1 and Figures S1–S5

Correspondence to:
G. Kulkarni,
Gourihar.Kulkarni@pnnl.gov

Citation:
Kulkarni, G., C. Sanders, K. Zhang, X. Liu, and C. Zhao (2014), Ice nucleation of bare and sulfuric acid-coated mineral dust particles and implication for cloud properties, *J. Geophys. Res. Atmos.*, *119*, 9993–10,011, doi:10.1002/2014JD021567.

Received 28 JAN 2014
Accepted 11 AUG 2014
Accepted article online 15 AUG 2014
Published online 29 AUG 2014

Ice nucleation of bare and sulfuric acid-coated mineral dust particles and implication for cloud properties

Gourihar Kulkarni[1], Cassandra Sanders[2], Kai Zhang[1], Xiaohong Liu[3], and Chun Zhao[1]

[1]Atmospheric Sciences and Global Change Division, Pacific Northwest National Laboratory, Richland, Washington, USA, [2]Environmental and Biological Sciences, Washington State University, Richland, Washington, USA, [3]Department of Atmospheric Sciences, University of Wyoming, Laramie, Wyoming, USA

Abstract Ice nucleation properties of atmospherically relevant dust minerals coated with soluble materials are not yet well understood. We determined ice nucleation ability of bare and sulfuric acid-coated mineral dust particles as a function of temperature (−25 to −35°C) and relative humidity with respect to water (RH_w; 75 to 110%) for five different mineral dust types: (1) Arizona test dust, (2) illite, (3) montmorillonite, (4) K-feldspar, and (5) quartz. The particles were dry dispersed and size selected at 200 nm, and we determined the fraction of dust particles nucleating ice at various temperatures and RH_w. Under water-subsaturated conditions, compared to bare dust particles, we found that coated particles showed a reduction in their ice nucleation ability. Under water-supersaturated conditions, however, we did not observe a significant coating effect (i.e., the bare and coated dust particles had nearly similar nucleating properties). X-ray diffraction patterns of the coated particles indicated that acid treatment altered the crystalline nature of the surface and caused structural disorder; thus, we concluded that the lack of such structured order reduced the ice nucleation efficiency of the coated particles in deposition ice nucleation mode. In addition, our single column model results show that coated particles significantly modify cloud properties such as ice crystal number concentration and ice water content compared to bare particles in water-subsaturated conditions. However, in water-supersaturated conditions, cloud properties differ only at warmer temperatures. These modeling results imply that future aged dust particle simulations should implement coating parameterizations to accurately predict cloud properties.

1. Introduction

Ice nucleation involving aerosol particles and solution droplets is an important process for the formation of ice crystals in cirrus and mixed-phase clouds. Mineral dust is one of the most abundant aerosol species in the atmosphere, and substantial evidence suggests that these particles are efficient ice nuclei (IN) [e.g., *Prospero et al.*, 1987; *DeMott et al.*, 2003; *Welti et al.*, 2009; *Kulkarni et al.*, 2009; *Kulkarni and Dobbie*, 2010]. In general, mineral dust particles can follow three possible pathways to induce ice nucleation; these are (1) deposition ice nucleation (i.e., ice formation directly from water vapor); (2) condensation/immersion freezing (i.e., freezing initiated by the IN located within the supercooled water or solution droplet); and (3) contact freezing (i.e., freezing that occurs at the moment when IN contacts a supercooled water droplet or solution droplet). The ice nucleating ability of a particle can depend on its composition, mixing state, [e.g., *Kanji et al.*, 2008; *Welti et al.*, 2009], and size [e.g., *Welti et al.*, 2009], as well as temperature and/or ice-saturation conditions.

Previously, researchers have shown that the ice nucleating ability of bare mineral dust particles can deteriorate if the particles are coated with soluble materials such as sulfuric acid [*Eastwood et al.*, 2009; *Chernoff and Bertram*, 2010; *Sullivan et al.*, 2010a; *Niedermeier et al.*, 2011; *Tobo et al.*, 2012; *Wex et al.*, 2013]. These studies, which are summarized in Table 1, indicate that coatings can block ice-active sites and therefore can inhibit the ability of dust particles to act as IN by increasing the ice-saturation conditions and/or lowering the freezing temperature required for ice nucleation.

Additionally, these studies suggest that the ice nucleating ability of coated dust particles depends upon mineralogy, the extent of the coating, and the source of the dust [*Cziczo et al.*, 2009; *Sullivan et al.*, 2010a; *Wex et al.*, 2013]. *Cziczo et al.* [2009] compared the ice nucleating properties of bare and coated particles of Arizona test dust (ATD) and illite minerals, and they found that only ATD particles are sensitive to the acid treatment. Note that ATD and illite minerals have different mineralogical compositions [*Broadley et al.*, 2012]. Further,

AGU Journal of Geophysical Research: Atmospheres 10.1002/2014JD021567

Table 1. Summary of Past Studies That Investigated the Influence of Sulfuric Acid Coating on the IN Activation Ability of Mineral Dust Particles at Temperature 0 to −40°C[a]

Reference	IN Investigation Technique	Mode of Ice Nucleation or Freezing	Temperature (°C)	Mineral Dust		Particle Generation Technique	Coating Confirmation Technique
				Type	Diameter (μm)		
Cziczo et al. [2009]	Expansion-type cloud chamber	Deposition, immersion, condensation	−20 to −45	ATD, Illite	< ~ 1	Dry particle suspension/generation	Fourier transform IR spectroscopy
Niedermeier et al. [2010]	Continuous flow cooling chamber	Immersion	−34 to −40	ATD	0.3	Dry particle suspension/generation	CCN activation, aerosol mass spectrometry
Niedermeier et al. [2011]	Continuous flow cooling chamber	Immersion	−28 to −40	ATD	0.3	Dry particle suspension/generation	CCN activation, aerosol mass spectrometry
Wex et al. [2013]	Continuous flow cooling chamber	Deposition, Immersion	−26, −30, and −34	Kaolinite	0.3	Dry particle suspension/generation	CCN activation, aerosol mass spectrometry
Sullivan et al. [2010a]	Continuous flow diffusion chamber	Deposition, immersion/condensation	−25 and −30	ATD	0.3	Dry particle suspension/generation	CCN activation, aerosol mass spectrometry
Tobo et al. [2012]	Continuous flow diffusion chamber	Deposition, immersion/Condensation	−26, −30, and −34	Kaolinite	0.3 and 0.7	Dry particle suspension/generation	CCN activation, aerosol mass spectrometry
Knopf and Koop [2006]	Optical microscope with a flow cell	Deposition	−13 to −76	ATD	0.7 to 10	Wet atomization	Assumption of spherical core shell model
Eastwood et al. [2009]	Optical microscope with a flow cell	Deposition	−27 to −40	Kaolinite	5 to 15	Wet atomization	Assumption of spherical core shell model
Chernoff and Bertram [2010]	Optical microscope with a flow cell	Deposition	−26 to −39	Kaolinite, Illite, Quartz, Montmorillonite	~ 7 to 10	Wet atomization	Assumption of spherical core shell model
Present study	Continuous flow diffusion chamber	Deposition, immersion/condensation	−25, −30, and −35	ATD, Illite, Montmorillonite, K-feldspar, Quartz	0.2	Dry particle suspension/generation	XRD

[a]Most of the studies focused on ATD, while many other atmospheric relevant minerals were not extensively studied. See text for details.

their single-particle mass spectrometry analysis revealed that particles might be partially coated, and Cziczo et al. suggest that these incomplete coatings expose unprocessed surfaces to induce ice nucleation under identical conditions to those of bare particles. Recently, *Wex et al.* [2013] examined ice nucleation properties of kaolinite particles from two different vendors: Fluka and Clay Minerals Society (CMS). They found that the coated particles from Fluka had poor ice-nucleating efficiency, whereas IN efficiency of bare and coated particles from CMS was similar. These results suggest that the particles from Fluka may have contained other minerals, such as potassium and feldspar, at the surfaces that were destroyed in the process of coating, thus reducing the ice-nucleating efficiency. *Knopf and Koop* [2006], however, did not observe a coating effect on ice-nucleating efficiency. They generated ATD particles using a process called wet atomization, in which water droplets containing particles were deposited on hydrophobic substrates and dried to obtain bare particles. This experimental procedure was repeated to generate sulfuric acid-coated particles, where 2 mg of ATD powder was suspended in a 0.005 wt % of the acid solution. This wet particle generation method can increase the wettability or hygroscopicity [e.g., *Herich et al.*, 2009; *Koehler et al.*, 2010; *Sullivan et al.*, 2010b] of the generated particles. Therefore, the wet particle generation technique can influence ice nucleation properties such that bare and coated particles may have similar ice-nucleating efficiencies.

Natural mineral dust particles are a complex mixture of different minerals (e.g., illite, kaolinite, quartz, and montmorillonite) [e.g., *Jeong*, 2008; *Shi et al.*, 2008; *Murray et al.*, 2012]. In contrast, the majority of previous studies (Table 1) have investigated the ice nucleation properties of only one or two minerals: ATD and kaolinite. One exception is the study of *Chernoff and Bertram* [2010], which investigated four different minerals (i.e., kaolinite, illite, quartz, and montmorillonite). ATD is composed of various mineral species [e.g., *Murray et al.*, 2012], but the ice nucleation properties of these different minerals that compose ATD are poorly understood. It was found that ATD is a more efficient IN than natural dust, and the mineralogy of ATD is significantly different from natural dust [*Broadley et al.*, 2012; *Murray et al.*, 2012; *Hoose and Möhler*, 2012]. This finding questions the use of ATD as a surrogate for atmospherically relevant mineral dust particles in laboratory experiments. In turn, this challenges the use of these measurements to develop ice nucleation parameterizations for cloud models. Some studies have generated polydisperse particles using the wet atomization technique described above [*Knopf and Koop*, 2006; *Eastwood et al.*, 2009; *Chernoff and Bertram*, 2010]. This technique could inadvertently modify the physical and chemical properties of bare particles before their ice nucleation properties are investigated [e.g., *Sullivan et al.*, 2010b]. Other studies [*Eastwood et al.*, 2009; *Chernoff and Bertram*, 2010; *Cziczo et al.*, 2009] have examined the onset temperature and saturation conditions of ice nucleation but not the ice-nucleated fraction.

Onset ice nucleation conditions of different particle types can be parameterized using single contact angles between the ice germ and the solid substrate for global climate models [e.g., *Liu and Penner*, 2005; *Hoose et al.*, 2010], but this approach should be used with caution in cloud modeling studies. Recent studies [e.g., *Ervens and Feingold*, 2012; *Wheeler and Bertram*, 2012] have shown that single contact angle parameterization is not suitable for representing ice nucleation processes. Recently, *Hoose and Möhler* [2012] suggested that, to improve the heterogeneous ice nucleation parameterizations, ice nucleation measurements should also report the ice-nucleated fraction of different size-selected minerals as a function of temperature and/or RH_w. From Table 1, we can see that deposition and condensation/immersion ice nucleation measurements performed under identical experimental conditions (i.e., particle size, particle generation technique, and coating mechanism) are missing for the sulfuric acid-coating effect.

A lack of consistent measurements motivated us to investigate ice nucleation properties of atmospherically relevant dust minerals (e.g., illite, montmorillonite, K-feldspar, and quartz), in comparison to ATD, at temperatures ranging from −25 to −35°C in water-subsaturated and water-supersaturated regimes under identical experimental conditions. These measurements are well suited for global climate models [e.g., *Liu and Penner*, 2005; *Hoose et al.*, 2010], in which dust mineralogy/speciation and their effects on ice nucleation [e.g., *Hoose et al.*, 2008] are now considered. In previous modeling studies, mineral dust was treated as a single-entity aerosol (i.e., representative of all dust minerals). Recent results that link ice nucleation properties to specific dust minerals (e.g., kaolinite and montmorillonite) show a significant impact on the modeled cloud water path and on cloud cover, especially at high altitudes [*Liu et al.*, 2013]. Globally transported dust minerals often are coated with secondary materials [e.g., *Kojima et al.*, 2006; *Sullivan et al.*, 2007; *Shi et al.*, 2008; *Fairlie et al.*, 2010]. Various processes, such as in-cloud processes [*Andreae et al.*, 1986], coagulation with sulfate particles [*Levin et al.*, 1996], and uptake of SO_2 on the surface and further oxidation of SO_2 by ozone

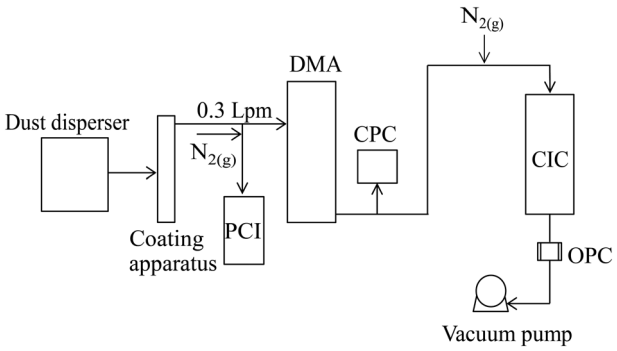

Figure 1. Schematic of the experimental setup. Dust particles were suspended in a dust disperser and passed through a coating apparatus that had a reservoir of sulfuric acid heated to either 100 or 150°C. Differential Mobility Analyzer (DMA) classified the particles of mobility diameter 200 nm that were transported to the PIXE Cascade Impactor (PCI), condensation particle counter (CPC), and compact ice chamber (CIC). CIC was connected to the optical particle counter (OPC) and further to the vacuum pump. Fraction of dust particles that nucleated ice was calculated using CPC and OPC measurements; see text for details.

[*Luria and Sievering*, 1991], can cause sulfate coating on atmospheric dust particles. Global aerosol model simulations show that the thickness of the sulfate coating can vary from 0 to 20% of the dust particle radius [*Liu et al*., 2005; *Bauer et al*., 2007]. Field studies at rural sites in the eastern United States by *Mamane and Noll* [1985] found that sulfate coating was on the order of 1 to 3% of the particle mass. These coating thickness estimates indicate that long-range transported dust particles in the atmosphere can acquire sufficient coating mass. Further, the coating material can affect the ice nucleating properties of dust particles [e.g., *Hoose et al*., 2008; *Hoose and Möhler*, 2012; *Girard et al*., 2013]. Cloud model simulations by *Girard et al*. [2013] show that sulfuric acid-coated dust particles can influence Arctic clouds. They reported that cloud microstructural properties, such as ice crystal concentration, ice, and liquid water paths, are sensitive to the ice nucleation properties of bare and coated particles. Further, they found that these two different effects had an impact on the radiation budget at the top of the atmosphere. Using a global climate model, *Hoose et al*. [2008] showed that coated mineral dust particles can affect mixed-phase cloud properties by reducing the ice water content and precipitation from these clouds. Their sensitivity simulations showed that these indirect effects on aerosol can increase the reflectance of solar radiation by increasing cloud cover and albedo. Therefore, it becomes important to understand and quantify the effect of coating on ice nucleation properties of aerosol particles in cloud models. As a result, in addition to the laboratory experiments, we also parameterized our ice nucleation measurements and examined the sensitivity of the cloud microphysical properties to the coating effect in a single-column model.

The goal of this study is to (1) investigate the ice nucleating properties of different bare and coated minerals under identical experimental conditions, (2) analyze chemical and microphysical properties of particle surfaces to further understand the measurements, and (3) perform modeling studies to understand the roles of bare and coated particles on cloud properties at water-subsaturated and water-supersaturated conditions. The ice nucleation parameterizations developed in this study can be applied to the cloud-modeling studies as, to our best knowledge, there are no such formulations available.

2. Experimental and Modeling Methodology

2.1. Particle Generation

Figure 1 shows the experimental setup used to investigate the ice nucleating properties of size-selected mineral dust particles. ATD (A1 Ultrafine test dust), illite, montmorillonite, quartz, and kaolinite mineral dust types were dry-dispersed using a dust disperser (dry powder dispersion; TSI, 3433). ATD and illite dust samples were purchased from Powder Technology Inc., and Clay Minerals Inc., respectively. The montmorillonite and kaolinite particles were purchased from Sigma-Aldrich Co. LLC, and the K-feldspar was obtained from Excalibur Mineral Inc. The chemical compositions, as provided by the vendors, are presented in Table S1 in the supporting information. The particles were coated with sulfuric acid in a coating apparatus [*Friedman et al*., 2011] that was maintained at a temperature of either 100°C or 150°C. In this unit, particles entered the glass tube and passed over a heated sulfuric acid bath. The bath section was heated using flexible heating tapes, and its temperature was controlled using a thermostat. The residence time of the particles within the tube was < 5 s, which was achieved by maintaining constant air flow (0.3 liter per minute (Lpm)) for all experiments. Coating thickness was roughly estimated based on a simple acid molecule condensation parameterization (Appendix A). We assumed acid molecules condensed for a short period and bulk vapor concentration was fixed at all times

during vapor condensation. We also assumed that particles were spherical with a homogeneous coating around them. At acid bath temperatures of 100°C and 150°C, our estimation showed coating thicknesses of less than 1 nm (2 monolayers) and 40 nm (80 monolayers) of acid molecules, respectively. We note that our assumptions affect the coating thickness estimates, such that these estimates could be higher than the actual coatings (Appendix A). We will refer to the particles coated at the lower temperature and the higher temperature as thin- and thick-coated particles, respectively. Coated particles with a mobility diameter of 200 nm were size selected by a differential mobility analyzer (TSI, 3080), and they were transported to the condensation particle counter (CPC) and compact ice chamber (CIC; section 2.3). We observed that the differential mobility analyzer produced multiple charged particles, but not a monodispersed particle distribution; therefore, large (multiple charged) particles (>200 nm) were also transmitted. Theoretical calculations [*Baron and Willeke*, 2001] indicate that double and triple charged particles were 324 nm and 440 nm in size, respectively. Using a sample flow rate of CIC and CPC measurements, the total numbers of particles or condensation nuclei (CN) available for IN measurements were calculated. For X-ray diffraction (XRD) analysis, the coated particles were diverted to the PIXE cascade impactor (Model I-1 L), where they were collected on carbon tape that was attached to the mounting support of stage L2. According to the impactor specifications, this stage had a particle diameter cut point between 0.25 to 0.12 μm. To confirm that we did not modify the physical and chemical properties of the dust particles due to the heating effect within the coating apparatus, we also collected (for XRD analyses) particles that had passed through the same coating apparatus, but with no sulfuric acid solution. The empty coating apparatus was maintained at either 100°C or 150°C.

2.2. XRD Analysis

XRD is an analytical technique that is widely used for the identification of a crystalline material and its structural state. MicroXRD data were collected using a Rigaku D/Max Rapid II instrument equipped with a 2-D image plate detector. X-rays were generated with a MicroMax 007HF generator fitted with a rotating Cr anode (Lambda = 2.2897 Å) and focused on the specimen through a 300 μm diameter collimator. Samples were dispersed on double-sided carbon tape on a flat-top sample holder. We used 2DP, Rigaku 2-D Data Processing Software (Version 1.0, Rigaku, 2007), to integrate the diffractions rings captured by the detector. We then performed an analysis of the diffraction data using JADE 9.5 (Materials Data, Inc.) and the PDF4+ 2012 database from International Centre for Diffraction Data (ICDD). We verified the correct sample-to-detector distance by measuring the lattice constant of a Si standard (Silicon powder, National Institute of Standards and Technology 640c). The observed lattice parameters deviated from the standard by 0.002 Å. We also determined lattice parameters and average crystallite sizes from Le Bail fitting in TOPAS v4.2 (Bruker AXS GmbH, Germany).

2.3. Ice Nucleation Experiments

We obtained ice nucleation properties of size-selected mineral dust particles using CIC. The working principle of CIC has been noted in the literature [*Stetzer et al*., 2008; *Friedman et al*., 2011; *Kulkarni et al*., 2012], but a brief description of its design details follows. The chamber consists of two vertical parallel plates with an evaporation section attached at the bottom of the chamber to remove water droplets [*Stetzer et al*., 2008]. A continuous flow water vapor diffusion chamber ensures that, when aerosol particles are placed between the layers of two sheath flows, they are exposed to constant temperature and relative humidity with respect to ice (RH_{ice}) over the length of the chamber. Saturation vapor pressures over ice and water are calculated using formulations published by *Murphy and Koop* [2005]. The chamber wall temperatures are controlled by using two external cooling baths (Lauda Brinkmann Inc.), and temperature data are logged using the National Instrument CompactRIO programmable automation controller (cRIO-9114 combined with cRIO-9022). The chamber plates are temperature controlled independently to develop a linear temperature gradient across them, which, according to the principle of thermal gradient diffusion theory, produces a RH_{ice} profile between the plates [e.g., *Rogers*, 1988]. At the beginning of the experiment, the chamber walls are coated with an ~0.5 mm thick ice layer, and the temperature gradient is set at zero, which creates ice-saturation conditions inside the chamber (RH_{ice} = 100%). Then, the refrigeration system cools one plate and warms the other to increase the RH_{ice}. The total flow used was 11 Lpm; sheath and sample flows used were 10 and 1 Lpm, respectively, which limits the aerosol residence time to ~12 s within the CIC. Ice nucleates on the aerosol particles, and the newly formed ice crystal grows to a size greater than the original aerosol size. Ice crystals at > 1.5 μm exiting the chamber are counted with an optical particle counter (OPC; CLiMET, model CI-3100). The ice active fraction (F_{ice}) was calculated as the ratio of number of ice crystals measured by the

OPC to the CN available for nucleation. Background IN concentrations were calculated to estimate the lower detection limit of F_{ice}. To calculate the background IN, we ran the CIC maintained at $RH_w = 110\%$ and three temperature conditions (−25, −30, and −35°C) conditions while sampling only filtered dry air for at least 30 min at the beginning, middle, and toward the end of the experiment. The lower detection limit of F_{ice} was 0.01%. To make sure that our background IN concentration was less than ~ 0.01%, we restricted our experiment duration time to less than 3 h.

These ice nucleation measurements were further analyzed using the concept of ice-active surface site (N_s) density theory. In this analysis, the ice-active sites are assumed to be distributed over the dust surface at a certain activation energy density, such that nucleation will occur at a particular site with a characteristic temperature and RH_{ice} [*Connolly et al*., 2009; *Murray et al*., 2012; *Niemand et al*., 2012]. According to equation (1) from *Niemand et al*. [2012], the density of N_s can be expressed as

$$N_s = -\frac{1}{A} 1n\{1 - F_{ice}(RH_{ice})\} \quad (1)$$

where A is the surface area per particle calculated, assuming dust particles are spherical in shape, and F_{ice} (RH_{ice}) is the fraction of ice particles observed as a function of RH_{ice}, as discussed above.

2.4. Cloud Modeling

We used the single-column mode of the Community Atmosphere Model CAM5.1 [*Neale et al*., 2010] to examine the sensitivity of cloud properties to ice nucleation on bare and coated particles, such as ice crystal concentration and ice water content, under both water-subsaturated and water-supersaturated conditions. The atmospheric column that we simulated is located at the Southern Great Plain (SGP) site near Lamont, Oklahoma. We used the National Oceanic and Atmospheric Administration's rapid update cycle analyses to derive the large-scale forcing terms for the model column using the constrained variation objective analysis approach described by *Zhang and Lin* [1997] and *Zhang et al*. [2001]. We used surface radiation and precipitation observed at the SGP site and top-of-atmosphere radiation measurements by the Geostationary Operational Environmental Satellite to adjust the atmospheric state variables to conserve column-integrated quantities such as mass, moisture, and static energy. In addition to ice nucleation treatment processes, the model also considers complex ice microphysical processes, such as water vapor deposition, ice sublimation, melting, autoconversion from cloud ice to snow, riming, accretion, and sedimentation.

The model has 30 vertical levels up to 10 hPa and a time step of 10 min. The ice cloud microphysics processes are described in *Liu et al*. [2012a, 2012b] and *Zhang et al*. [2013]. The simulation was performed for the month of April 2010 during the period of the Department of Energy (DOE) Small Particles in Cirrus (SPARTICUS) field campaign [*Zhang et al*., 2013], with a spin-up period of three model days.

3. Results and Discussion

3.1. XRD Analysis

The XRD patterns of four bare and coated dust types are shown in Figure 2. Different peaks or degrees 2 theta (2θ) reflections indicate the crystalline structure or characteristic identities of different minerals presented within each dust type [e.g., *Panda et al*., 2010; *Melo et al*., 2010; *Volzone and Ortiga*, 2011]; that is, each peak corresponds to one mineral (for convenience, we name them as minor minerals). Several minor minerals were detected and quantified, as shown and listed in Figure 2 and Table 2, respectively. Particles from each dust type were mostly composed of various minor minerals such as illite1, illite2, montmorillonite, quartz, calcite, albite, anorthite, and orthoclase. Albite and orthoclase, from the K-feldspar group, were found to be common minor minerals in ATD and illite. In ATD, the compositions of albite and orthoclase were found to be 8 and 12%, respectively. Illite was primarily composed of illite2 and quartz, with only ~ 3% of orthoclase. A recent study [*Murray et al*., 2012] showed that the K-feldspar group minerals are common minerals found in most atmospheric mineral dust particles and estimated that, on average, ~ 10% of atmospheric dust is composed of K-feldspar minerals.

The XRD patterns of bare particles showed a number of intense peaks, indicating that these particles are crystalline in nature [*Warren*, 1990; *Cullity and Stock*, 2001]. Once the particles were coated with sulfuric acid, the peak intensity of some of these minor minerals decreased significantly, indicating that the particles were amorphous in nature. For example, the positions of 2θ reflections in the region between $30° < 2\theta < 35°$ for

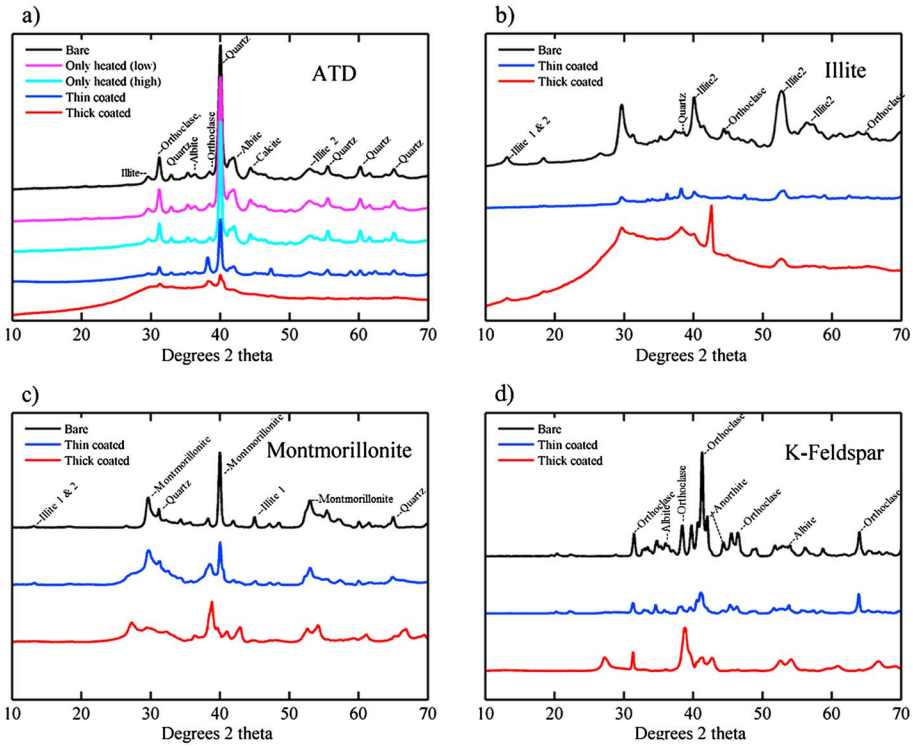

Figure 2. XRD of bare and acid treated (coated) mineral dust particles. Crystallographic properties of some minerals are listed in Table 3.

ATD were found to decrease after coating, and well-defined peaks in this region were not observed. In this sample, we also observed that the calcite mineral ($43° < 2\theta < 47°$) was completely lost after coating. The XRD patterns of the bare and coated quartz particles were nearly identical (Figure S1). However, for thickly coated particles, we observed a peak at $2\theta = \sim 42°$, which could be from a new phase that had formed on the surface. It was not possible to identify the mineral associated with this peak, but we speculate that any minor impurities (nonquartz minerals undetected by XRD) that were sensitive to the high acid concentration could have produced these compounds.

Table 2. Chemical Composition of Minor Minerals From XRD Analyses

Dust Type	Weight %	Minerals and Chemical Formula
ATD	25	Quartz–SiO_2
	3	Calcite–$Ca(CO_3)$
	8	Albite–$Na(Si_3Al)O_8$
	12	Orthoclase–$KAlSi_3O_8$
	51	Illite2–$(K,H_{30})Al_2\ (Si_3Al)O_{10}(OH)_2.xH_2O$
Illite	--	Illite1–$KAl_2(Si_3Al)O_{10}(OH)_2$
	85	Illite2–$(K,H_{30})Al_2\ (Si_3Al)O_{10}(OH)_2.xH_2O$
	3	Orthoclase–$KAlSi_3O_8$
	10	Quartz–SiO_2
	--	Albite–$Na(Si_3Al)O_8$
Montmorillonite	48	Montmorillonite–$(Ca,Na)_{0.3}Al_2(Si,Al)_4O_{10}(OH)_2.xH_2O$
	32	Illite1–$KAl_2(Si_3Al)O_{10}(OH)_2$
	--	Illite2–$(K,H_{30})Al_2\ (Si_3Al)O_{10}(OH)_2.xH_2O$
	8	Quartz–SiO_2
K-Feldspar	33	Orthoclase–$KAlSi_3O_8$
	29	Albite–$(Na,Ca)Al(Si,Al)_3O_8$
	37	Anorthite–$(Ca,Na)(Al,Si)_2Si_2O_8$
Quartz	100	Quartz–SiO_2

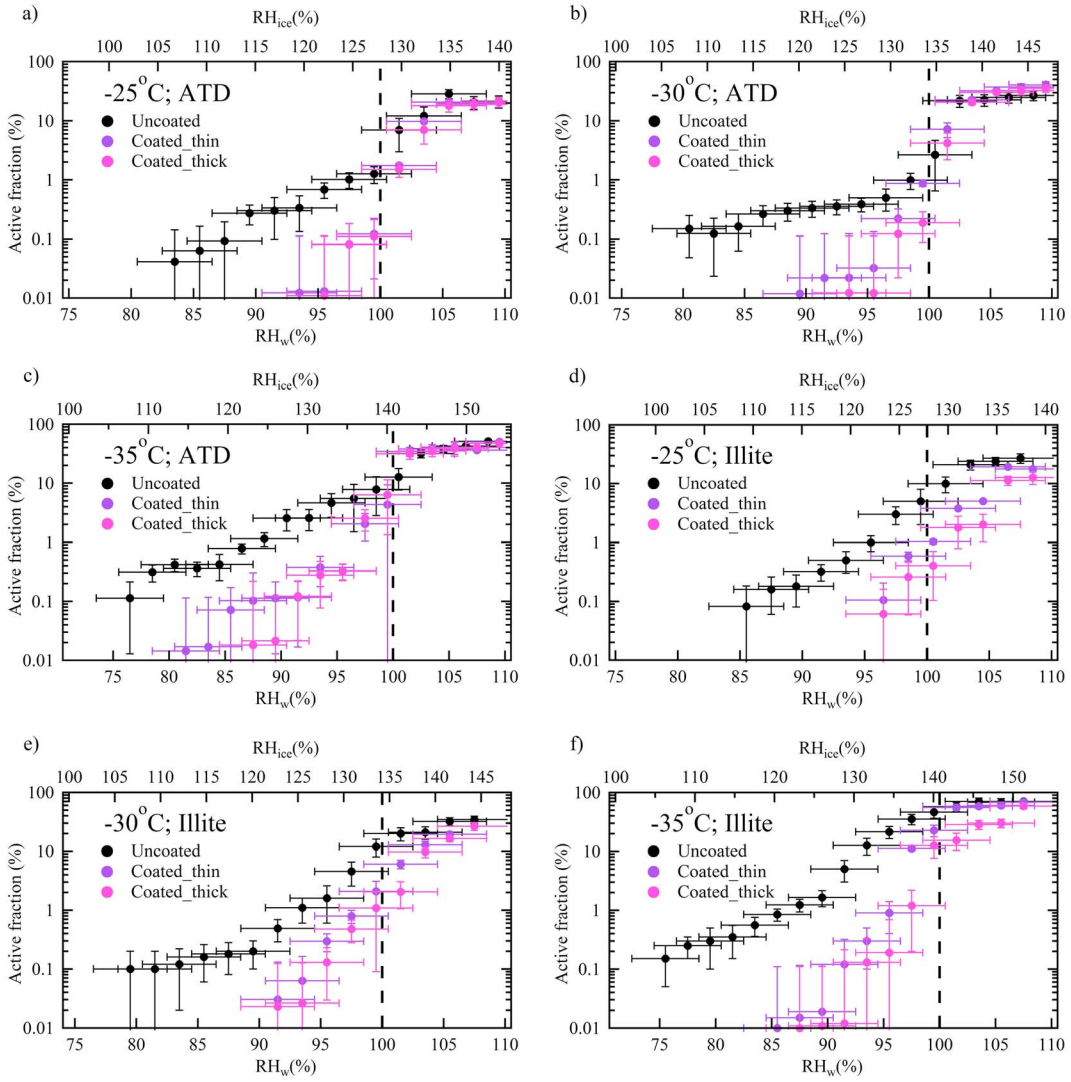

Figure 3. Ice active fractions of 200 nm bare and coated ATD particles at −25, −30, and −35°C as a function of RH_w and RH_{ice}. (a to c, d to f, g to i, and j to l) Results for ATD, illite, montmorillonite, and K-feldspar, respectively. See text for details. Vertical dashed line indicates the water saturation line. The vertical errors bars are equal to the one standard deviation of the measurements ($n = 8$). The horizontal error bars are equal to the ±3% uncertainty in the RH_w measurements.

In addition, the XRD patterns of the heated ATD particles are shown in Figure 2a. We observed negligible structural changes. For example, peaks such as illite2, orthoclase, albite, and calcite are clearly visible, and their intensities are very similar to bare particles. These results confirm that we did not inadvertently modify the physical and chemical properties of the dust particles before their ice nucleating properties were investigated. However, we cannot neglect any additional chemistry that may have occurred if the hot sulfuric acid vapors had condensed on the dust particle.

3.2. Ice Nucleation Measurements of Bare and Coated Mineral Dust Particles

Figure 3 shows the F_{ice} of four bare and coated mineral dust species, (1) ATD, (2) illite, (3) montmorillonite, and (4) K-feldspar, as a function of RH_w and RH_{ice} at different temperatures: −25, −30, and −35°C. This figure shows the fraction of particles that induce ice nucleation in the deposition mode (water-subsaturated conditions; $RH_w < 100\%$) and the condensation/immersion freezing mode (water-supersaturated conditions; $RH_w \geq 100\%$). We assume that only deposition ice nucleation occurs at water-subsaturated conditions. However, we also note that a recent study [*Marcolli*, 2014] hypothesized that condensation freezing may be

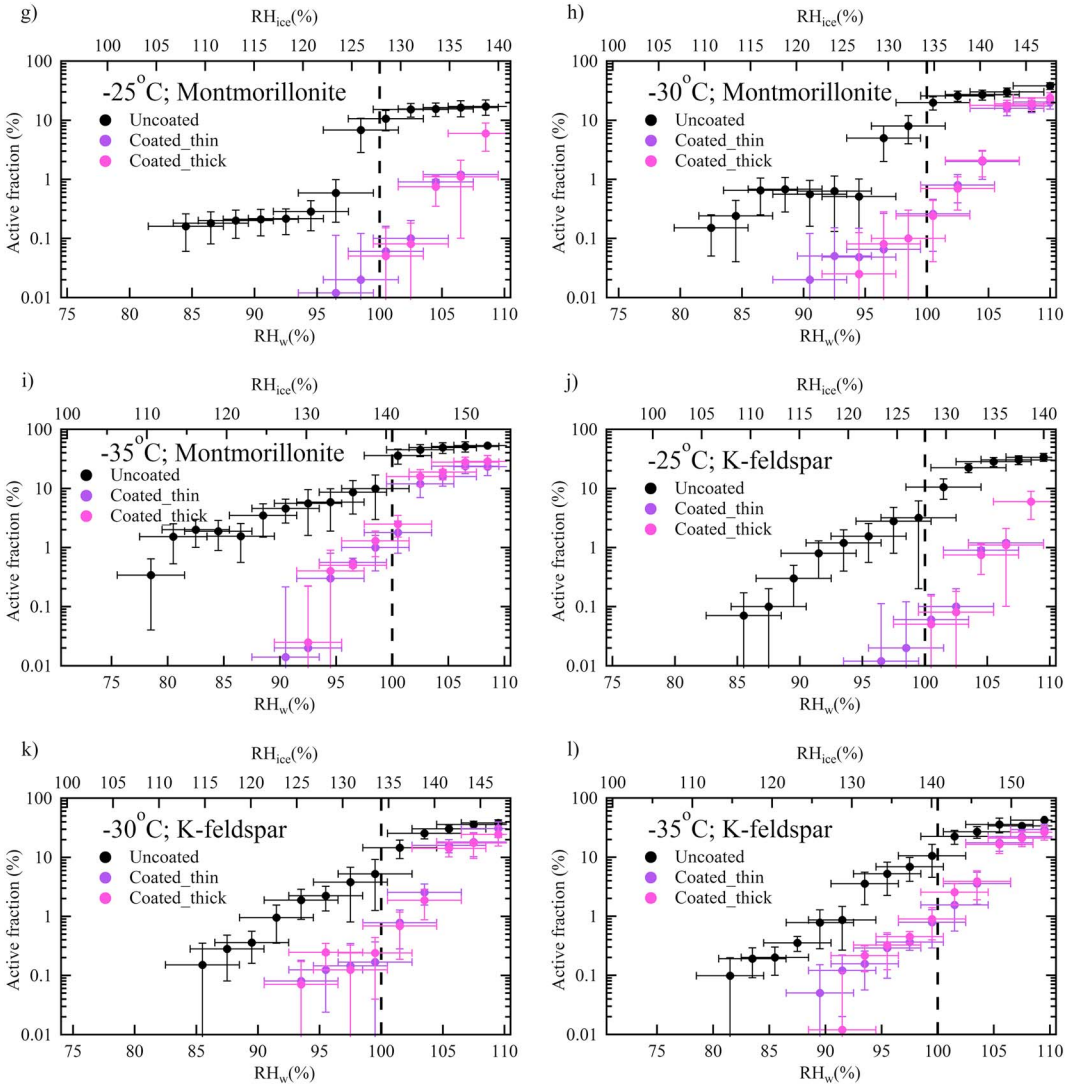

Figure 3. (continued)

occurring at water-subsaturated conditions. The vertical error bars shown in the figure are equal to the one standard deviation of the measurements ($n = 8$), and the horizontal error bars are equal to the ±3% uncertainty in the RH_w measurements.

F_{ice} spectra, which represent the measurement of ice nucleation behavior, varied depending on temperature and RH_w (Figure 3). At water-subsaturated conditions, our results indicate that F_{ice} increases with increasing RH_w, which is in agreement with many previous studies that have also observed this ice nucleation behavior for dust particles [e.g., *Welti et al.*, 2009; *Sullivan et al.*, 2010c; *Tobo et al.*, 2012; *Kanji et al.*, 2013]. We observed (Figure 3) that all dust species at −25 and −30°C initiate ice at ~85% and ~80% conditions, respectively. However, at a lower temperature (−35°C), ice nucleation on ATD and illite particles was observed at RH_w = ~77%, and on montmorillonite and K-feldspar minerals at ~80%. At water-subsaturated conditions, the IN abilities of acid-treated particles was found to be lower compared to uncoated particles (Figure 3). The sensitivity at −25°C was so acute that ice nucleation was observed only near water saturation conditions. At the other two temperatures considered, (−30 and −35°C), the minimum RH_w required for ice nucleation onto dust particles was ~90% (including error limits). At water-supersaturated conditions, where particles are immersed in water droplets, changes in F_{ice} are also observed. We observed that a maximum F_{ice} is reached at −35°C for all four dust species: at 105% RH_w conditions, the F_{ice} of ATD

particles at −25, −30, and −35°C are ~ 20%, 22% and 35%, respectively. Under these conditions, the results also show that the F_{ice} values for bare and coated dust species are very similar.

The sensitivity of bare dust species to temperature and ice-saturation conditions can be attributed to the variability in the efficiency of active sites present on their surfaces that promote ice embryo formation as previously reported; e.g., by *Marcolli et al*. [2007]. *Marcolli et al*. [2007] found that, for dust particles with a diameter of at least 100 nm, nucleated ice consists of one active site on average, and they suggested that ice nucleation occurs on active sites that have a certain probability distribution. This suggests that active sites are required to nucleate ice, and according to *Pruppacher and Klett* [1997] the rate of ice embryo formation at these sites rises either with an increase in humidity at any particular temperature or with a decrease in temperature at fixed humidity conditions. Our result shows that at 85% F_{ice} was ~ 0.1%, and near the water saturation condition, F_{ice} increased from 1 to 10%, depending on the temperature. These results suggest that the dust particles tested here had varying a quality of active sites, such that some sites induced ice nucleation at lower and some at higher ice-saturation conditions.

Except for quartz particles, the IN abilities of acid-treated particles were found to be lower compared to bare particles in the deposition mode of ice nucleation. The sensitivity at −25°C was so strong that ice nucleation was observed only near water saturation conditions. At the other two temperatures (−30 and −35°C), the minimum RH_w required for ice nucleation on dust particles was ~ 90% RH_w (including error limits). In the condensation/immersion freezing conditions (particularly above $RH_w = 105\%$), coated particles did not show a significant decrease in the IN ability compared to bare particles. These observations are in agreement with *Sullivan et al*.'s [2010c] findings, which suggested that, at water-supersaturated conditions, surface chemical reactions might not change the original ice nucleating properties permanently because coating material could be removed by dissolution and could potentially expose surface active sites. These sites may induce ice nucleation via condensation freezing, and they showed that, in this freezing regime, ice nucleation properties of dust particles depend on the dust composition and the uptake mechanisms of condensed soluble materials. Additionally, they suggested that surface chemical reactions may lead to reaction products with different solubility levels. For example, *Panda et al*. [2010] concluded that sulfuric acid-treated kaolinite particles can result in a reaction product (i.e., aluminum sulfate) that can be easily dissolved in water. We speculate that such soluble reaction products might have been produced in our experiments and may be the reason that we did not observe the influence of a coating in this regime.

Thin- and thick-coated dust particles had very similar ice nucleating behaviors (Figure 3) in both the deposition and the condensation/immersion ice nucleation modes. This result suggests that condensation of sulfuric acid vapor occurring on the dust particles when the coating apparatus was maintained at 100°C was sufficient to modify the surface so that further condensation of vapor has no effect on ice nucleation efficiency of coated particles.

In general, acid coating leads to the dissolution or fragmentation of surface layers, ultimately modifying the surface. Recently, *Reitz et al*. [2011] suggested that chemical reactions between sulfuric acid and ATD particles reduced the hydrogenated fragments of the sulfate species and produced reaction products such as metal and ammonium sulfates. Sulfate anions can adsorb to these reactions products due to strong electrostatic attractions and modify the structural properties [e.g., *Stumm*, 1992]. It should also be noted that dust minerals undergo various structural changes, depending on the concentration of the acid. At lower acid strengths, there is an exchange between the cations of the dust and H^+ ions of the sulfuric acid [*Volzone et al*., 2005; *Volzone and Ortiga*, 2006; *Zhao et al*., 2013]. At a higher acid concentration, metallic ions can leach out from the interlayer structure of the dust minerals and may alter the structural and crystallite properties completely [*Panda et al*., 2010; *Makó et al*., 2006; *Rajesh et al*., 2008; *Volzone et al*., 2005; *Volzone and Ortiga*, 2011].

We performed XRD experiments (section 3.1) to identify any particular reasons for the decrease in the IN ability of the coated dust particles in the deposition ice nucleation mode. In our experiments, we clearly observed that the acid treatment distorted the atomic positions and thus modified the structural order. We know that large crystallographic differences or dislocations or structural disorderliness at the ice-substrate interface will increase the interface free energy and can reduce the ability of the dust particle to induce ice formation [*Pruppacher and Klett*, 1997]. To quantify these crystallographic effects, we calculated crystallographic properties such as lattice

Table 3. Crystallographic Properties: Lattice Parameters and Crystallite Sizes of Some Dust Particles (Bare and Coated) From XRD Analyses[a]

		Lattice Parameters (Å)			
Dust Type		*a*	*b*	*c*	Size (nm)
Montmorillonite (bare)		5.187(9)	8.935(16)	14.899(14)	3.8(1)
Montmorillonite (coated)		5.446(8)	9.034(15)	13.924(20)	2.8(1)
Quartz (bare)		4.918(5)	---	5.413(4)	50(3)
Quartz (coated)		4.927(8)	---	5.421(5)	33(2)
	Orthoclase	8.521(1)	12.944(5)	7.194(1)	40.4(6)
K-feldspar (bare)	Albite	8.173(6)	12.877(8)	7.081(4)	26(1)
	Anorthite	8.179(1)	12.856(3)	14.16(3)	41(1)
	Orthoclase	8.539(11)	12.906(28)	7.209(22)	40(5)
K-feldspar (coated)	Albite	8.200(10)	12.930(13)	7.093(45)	16(6)
	Anorthite	8.174(16)	12.853(20)	14.157(23)	37(4)
Ice-*I*h		4.52	--	7.36	--
AgI		4.592	--	7.51	--

[a]For comparison lattice parameters of ice-*I*h and efficient IN AgI are also shown. Uncertainties are presented in brackets, should be read ± of the last decimal (e.g., accuracy of *a* lattice parameter in montmorillonite (bare) is read as 5.187 ± 0.009).

parameters and crystallite sizes of montmorillonite and K-feldspar (Table 3). The results show that the crystal lattice dimensions of bare and coated dust particles do not match. For example, the length of the lattice parameters or the lattice constants—*a*, *b*, and *c*—of bare and coated montmorillonite are 5.187, 8.935, 14.899 and 5.446, 9.034, 13.924, respectively, in Å. The montmorillonite also consists of quartz, and the lattice parameters of bare and coated quartz were identical; this is expected because quartz does not react with acid (Figure S1). For comparison, we also tabulated the lattice parameters of ice-*I*h and AgI. Numerous previous studies [e.g., *Baklanov et al*., 1991; *Edwards and Evans*, 1960; *Vonnegut*, 1947] have shown that AgI is efficient IN because the crystal lattice closely matches ice-*I*h, indicating the importance of crystallographic properties on the IN ability of aerosol particles. The crystallite size of the minerals, which is the measure of the average size of a single crystal, was observed to decrease after acid treatment. For example, the crystal sizes of bare and coated montmorillonite particles were 3.8 and 2.8 nm, respectively. Detailed discussions of the influence of lattice fits on heterogeneous ice nucleation are beyond the scope of this paper.

In summary, our observations show that the acid treatment caused structural deformation or disorderliness in four dust test samples (ATD, illite, montmorillonite, and K-feldspar) (Figure 2 and Table 3), but the acid treatment did not modify the structural properties of the quartz particles (Figure S1 and Table 3). Acid treatment affected the K-feldspar group minerals (albite, orthoclase, and anorthite; Figure 2), which are suggested to be the important ice nucleating minerals for atmospheric ice nucleation [*Atkinson et al*., 2013; *Yakobi-Hancock et al*., 2013]. The peak intensities of the orthoclase and albite minerals were reduced in ATD, whereas the orthoclase from illite was completely lost. K-feldspar also showed a similar sensitivity toward acid treatment. The intensity of all three minor minerals was reduced, and the peaks were broad. These structural changes indicate that the ice nucleation sites of these commonly observed minor minerals in the test dust species were modified. These results indicate that destruction of the structured order led to the reduction of the ice nucleating properties of various dust species (Figure 3), but only at water-subsaturated conditions. These conclusions are in agreement with the experimental spectroscopic studies reported by *Yang et al*. [2011], in which they reported that ordered structures at dust (i.e., mica) surfaces are important for ice nucleation. In their experiments, they found that structured order becomes distorted or particle surface become amorphous with exposure to sulfuric acid. Ice nucleation experiments were not performed, but their study provides molecular-level insights into why dust particles coated with sulfuric acid are poor IN.

Previously, *Sullivan et al*. [2010a] reported that heated bare particles (ATD) had a minimal influence on IN properties (within experimental uncertainties), in both the deposition and condensation/immersion freezing modes. In their experiments, the authors used a thermodenuder to heat the particles, where temperatures were maintained at 45, 70, 85, or 250°C, and the residence time of the particles was 4 to 5 s. In our experimental setup, the coating apparatus was maintained at 100 or 150°C, and the flow was 0.3 Lpm, which

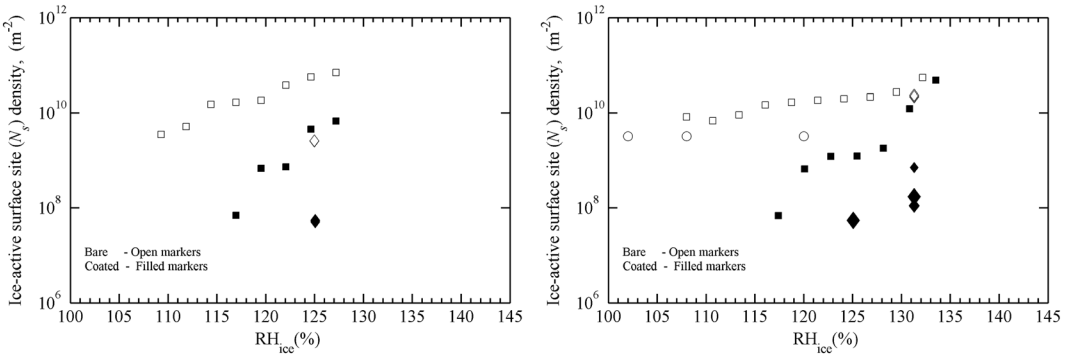

Figure 4. Comparison of ice nucleating properties of ATD particles in the water-subsaturated (or deposition ice nucleation) regime for temperature (left) −25°C and (right) −30°C. Square, diamond, and circle symbols represent data from present study, *Sullivan et al*. [2010a], and *Cziczo et al*. [2009], respectively. *Cziczo et al*. [2009] did not report ice nucleation properties for coated ATD particles. *Sullivan et al*. [2010a] data (Figure 4, left) display N_s densities from two experiments where they varied the temperature of coating apparatus to vary the coating mass material, no differences are observed. Whereas at −30°C the variability was observed; larger marker size corresponds to higher temperature of coating apparatus.

limited the particle residence time to ~ 5 s. In our study, we observed very little effect of only heated particles on ice nucleation properties (not shown; F_{ice} spectra of heated and bare particles was very similar, as shown in Figures 3a–3c). In addition to measuring the ice nucleating properties of heated dust particles, we also subjected these particles to XRD analysis and found that heat treatment caused negligible surface modifications (Figure 2a). On the other hand, we noted that hot sulfuric acid vapors within the coating apparatus may influence the chemical and physical properties of the dust particles. This possibility should be investigated in future studies.

3.3. Comparison of Ice Nucleation Properties With Previous Studies

The direct comparison of our results with previous investigations is difficult because of differences in the ice crystal detection threshold, nucleation mechanism, experimental setup, and the particle generation method. As a result, we calculated the N_s density (Figures 4 and 5) for comparison, as discussed in section 2.2. Figure 4 displays the N_s densities for the ATD particles calculated in the deposition mode at two different temperatures: −25 and −30°C. Our measurements indicate that the N_s densities for bare particles are higher than those for coated particles. Data reported by *Sullivan et al*. [2010a] also show that bare particles had higher N_s densities. However, their coated N_s densities are at least an order of magnitude smaller than those from our study at −25 and −30°C. At −30°C, however, the N_s densities for bare particles are in better agreement. Additionally, our results are in agreement with those of *Cziczo et al*. [2009] for bare particles at lower humidity conditions ($RH_{ice} < 110\%$; Figure 4, right), but at $RH_{ice} = 120\%$, our data are an order of magnitude smaller than theirs.

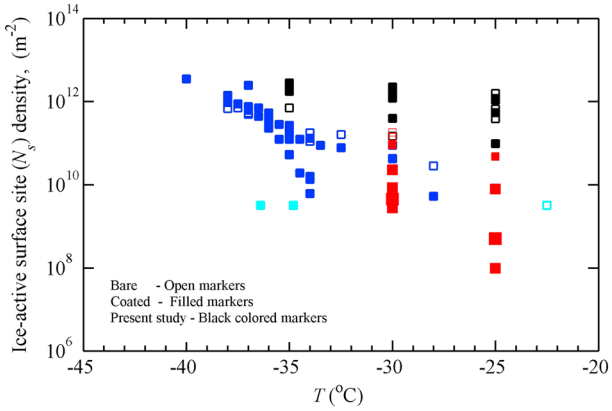

Figure 5. Ice-active surface site (N_s) densities for ATD particles in the immersion/condensation freezing conditions. The data sources are red, cyan, and blue color markers represent the data from *Sullivan et al*. [2010a], *Cziczo et al*. [2009] and *Niedermeier et al*. [2010, 2011], respectively. Size of markers shown for *Sullivan et al*. [2010a] data is correlated to the coating apparatus temperature. Small, middle, and large sizes correspond to the 45, 70, and 85°C.

Figure 5 shows the N_s densities calculated for the condensation/immersion freezing. We did not observe significant N_s density differences between the bare and coated particles at −25, −30, and −35°C. *Niedermeier et al*. [2010, 2011] also reported similar results, but only at temperatures lower than −32°C. At warmer temperatures of −30 and −28°C, they showed that bare and coated

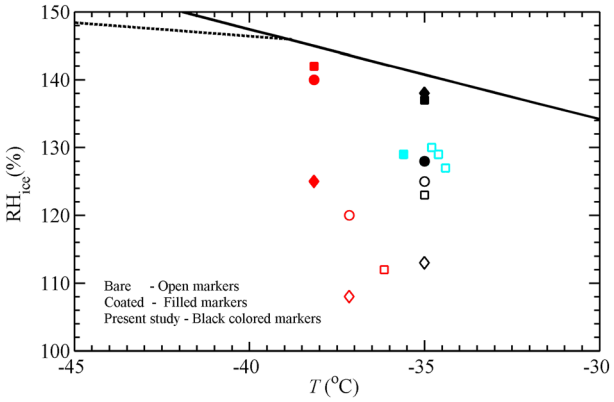

Figure 6. Critical RH_{ice} at which 1% of illite (square marker), montmorillonite (diamond marker) and quartz (circle marker) particles were activated in the water-subsaturated regime. Red and cyan color markers represent the data from *Chernoff and Bertram* [2010] and *Cziczo et al.* [2009], respectively. The water saturation line (solid) and a threshold line (dashed) for homogeneous ice nucleation for 200 nm solution droplet using a frozen fraction of 1% [*Koop et al.*, 2000] are also shown.

particles had different N_s densities. At −25°C, *Sullivan et al.* [2010a] reported 3 orders of magnitude variability in the N_s values calculated for coated particles, while, at −30°C, they observed a variability of 2 orders of magnitude.

Figure 6 shows the critical RH_{ice} required to activate 1% of the illite, montmorillonite, and quartz particles at −35°C. Results from the study by *Chernoff and Bertram* [2010] are also plotted. Our results show that coated particles require higher RH_{ice} conditions, which are in agreement with the results of *Chernoff and Bertram* [2010] study. Illite particles were investigated by *Cziczo et al.* [2009], and their data show a negligible influence of coating. However, their data are in agreement with our results for coated particles (illite).

The majority of previous studies report a decrease in the ice nucleation activity of particles coated with sulfuric acid (Table 1), and our measurements agree with those findings. In general, previous studies [*Niedermeier et al.*, 2011; *Wex et al.*, 2013; *Sullivan et al.*, 2010a; *Tobo et al.*, 2012; *Eastwood et al.*, 2009; *Chernoff and Bertram*, 2010] concluded that condensed sulfuric acid could react with and alter the mineral particle's surface properties, thus reducing the efficiency of ice nucleation active sites that are needed to nucleate the ice embryo in deposition ice nucleation mode. Our XRD results (note that these previous studies did not conduct XRD analysis) confirm that the physical and chemical properties of the surfaces are modified. This may be the reason that coated particles have lower ice nucleation efficiency in the deposition mode. On the other hand, *Knopf and Koop* [2006] reported that coating does not influence the ice nucleation properties of ATD particles. They suggest that these dust species, which are a complex mixture of different minor minerals, may or may not be reactive toward sulfuric acid. However, *Cziczo et al.* [2009] found that coating was more effective for ATD particles, but for illite particles, it was less pronounced. The degree of surface modification also may depend upon the amount of acid coating. For example, in the immersion freezing mode, *Niedermeier et al.* [2010] found that ATD particles coated with small amounts of acid could efficiently act as IN at higher temperatures, compared to particles that had larger amounts of the coating. More recently, *Wex et al.* [2013] suggested that surface morphology and composition could be important. They observed that kaolinite particles from two different sources showed different sensitivities toward ice nucleating ability in the immersion freezing mode: particles from one source showed that coating reduces the IN ability, while particles from another source showed no such reduction in the IN ability. Thus, past studies also demonstrate that mineralogy and a sufficient amount of coating to alter the particles' surfaces are important factors that can control the ice nucleation efficiency of acid-treated dust particles.

In addition, a number of previous studies examined the influence of mineral dust treated with various compounds (nitric acid, organics and ammonium sulfate) on their ice nucleation efficiency. The effect of nitric acid coating on ice nucleation ability of ATD particles was investigated by *Sullivan et al.* [2010a], which found that coating suppressed ice nucleation activity at water-subsaturated conditions, but observed no effect above water saturation. The influence of organic-coated dust particles showed that water saturation conditions are mostly required to nucleate ice [*Koehler et al.*, 2010; *Möhler et al.*, 2008]. Recently, *Tobo et al.* [2012] examined the effect of levoglucosan and sulfuric acid coatings on the ice nucleating properties of kaolinite particles. They observed that, at water-subsaturated conditions, the coating treatment reduced the ice nucleating ability of the kaolinite; however, at water-supersaturated conditions, only sulfuric acid coated dust particles showed a reduction in ice nucleation efficiency. Levoglucosan is a non-reactive material compared to sulfuric acid, which reacts vigorously with dust minerals, and their study suggests surface chemical reactions play an important role toward inducing ice formation on aged particles. Immersion

freezing experiments by *Niedermeier et al*. [2011] showed that the ice nucleation ability of sulfuric acid-coated dust particles was reduced compared to bare particles. These studies at water saturation conditions indicate that the sulfuric acid-treated dust particles had poor ice nucleation efficiency compared to bare particles. The immersion freezing efficiency of the aqueous solutions of ammonium sulfate compounds containing dust minerals was investigated by *Zobrist et al*. [2008] and *Zuberi et al*. [2002]. Their results also suggested that the ice nucleation efficiency of coated dust particles were significantly reduced.

3.4. Sensitivity of Cloud Microphysical Properties to Ice Nucleation on Bare and Coated Particles

Using Single column mode Community Atmospheric Model version 5, we investigated the influence of coated particles on the ice crystal number concentration and the ice water content in clouds. The IN concentrations were parameterized using the N_s density approach (section 2.3) at water-subsaturated and -supersaturated conditions. For these calculations, we used illite particles as a surrogate for natural dust particles, because illite has been shown to be an abundant mineral component observed in atmospheric dust particles [from *Murray et al*., 2012, Figure 5]. Figure S3 shows N_s density fits as a function of RH_{ice} at different temperatures for the deposition nucleation (a to c), and at $RH_w = 105\%$ for the condensation/immersion freezing (d). These temperature and RH_{ice}-dependent parameterizations were used to simulate the deposition and condensation/immersion freezing modes, respectively.

The model is configured such that particles can induce ice formation via deposition ice nucleation parameterization where there are no cloud droplets in the model grid box or via the condensation/immersion freezing mode when there are cloud droplets and the air is saturated with respect to water ($RH_w > 100\%$). The initial number concentrations of bare and coated illite particles are prescribed as $200\,L^{-1}$. In all these idealized simulations, both the bare and coated illite particles are assumed to be monodisperse and have a diameter of 200 nm. N_s density parameterizations were used to calculate the heterogeneous ice nucleation rate. We note that the simulated ice-number concentrations cannot be directly compared to the observations; however, the model sensitivity to different N_s densities derived from the laboratory experiments will provide insight on how the changes in ice nucleation activity of dust particles due to coating will affect the ice cloud properties in the atmosphere.

Figure 7 shows the simulated monthly mean vertical profiles of the ice crystal number concentration and the ice water content at the SGP site during April 2010. At water-subsaturated conditions, the maximum monthly mean ice crystal number concentration for both bare and coated cases was observed at ~ 450 hPa. Compared to the coated case, the modeled ice crystal number for the bare case was about 1 order of magnitude higher at each level. At water-supersaturated conditions, the modeled ice crystal number and ice water content are higher in the bare case than in the coated case. However, the difference between the bare and coated case above 600 hPa is much smaller. This is mainly due to that fact that the relative difference between the N_s densities of bare and coated illite particles is smaller at lower temperatures (Figure S3d), and the water-saturated air appears less frequently in the upper troposphere.

In the ice cloud regime, coated dust particles will lead to fewer nucleated ice crystals; thus, air can be supersaturated more easily because less water vapor is consumed. As a result, homogeneous ice nucleation can happen more easily in the upper troposphere (below −38°C), promoting the formation of small ice crystals. The actual impact on radiation will depend on how frequently the homogeneous ice nucleation occurs, which is further dependent on the updraft velocity and water vapor fluctuation in this region. In the mixed-phase cloud regime, where both cloud droplets and ice crystals exist, the smaller number of nucleated ice crystals from coated dust particles leads to a weaker Bergeron process, so the liquid water content would be higher than for the uncoated case. This would further delay the initiation of precipitation and increase the lifetime of the mixed-phase clouds, which leads to higher cloud albedo and larger shortwave cloud forcing.

Recently, *Girard et al*. [2013] performed cloud modeling studies to assess the effect of sulfuric acid-coated kaolinite dust particles on Arctic clouds and radiation budget. These authors calculated single contact angles for bare and coated particles and simulated the resulting numbers of ice crystals in a model using Classical Nucleation Theory. Girard et al. also observed that coated particles significantly modified the mixed-phase and ice cloud properties. Under mixed-phase cloud condition coated-particle simulations, there was an increased frequency of liquid water content, indicating very few ice crystals formed, whereas at ice cloud conditions (> −40°C), coated particles that nucleated liquid water froze homogeneously, and thus increased the ice water content.

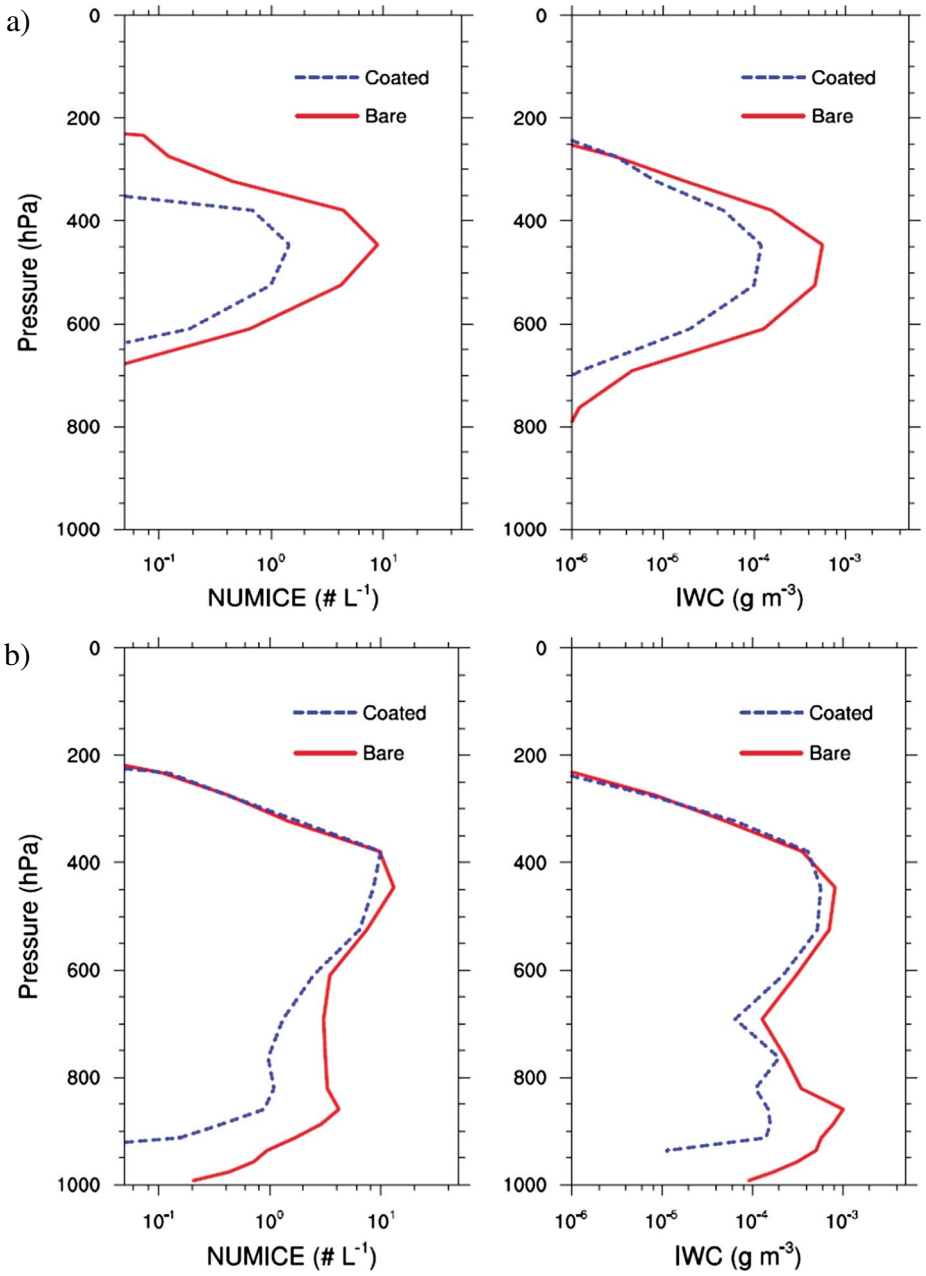

Figure 7. Monthly mean profile of the ice crystal number concentration (NUMICE) and ice water content (IWC) over the ARM SGP site in (a) deposition ice nucleation mode and (b) condensation/immersion freezing mode. Monthly profiles of these cloud properties are shown in Figures S4 and S5.

4. Summary and Atmospheric Implications

Mineral dust particles emitted from regions such as the Sahara and Asian deserts can be coated with secondary materials (e.g., sulfates, organics, and nitrates), away from the sources during their long-range transport. In this study, the ice nucleation properties of bare and sulfuric acid-coated dust particles were experimentally investigated in the deposition and condensation/immersion freezing modes at three different temperatures: −25, −30, and −35°C. We investigated five different dust mineral types, (1) ATD, (2) illite, (3) montmorillonite, (4) K-feldspar, and (5) quartz, at a diameter 200 nm. To generate coated particles, the bare particles were passed through a coating apparatus where the sulfuric acid bath was maintained at either 100 or 150°C. To understand the chemical and physical properties of coated particles compared to bare

particles, we performed XRD analyses of both mineral states. In addition, we investigated the ice microphysical sensitivities to ice nucleation on bare and coated particles in a single-column model.

Bare minerals induced ice formation in both the deposition and condensation/immersion freezing modes. At −25 and −30°C, these minerals required $RH_w > \sim 85\%$ to nucleate ice, whereas at −35°C, ice nucleation was observed for an RH_w as low as 80%. Except for quartz, the coated minerals exhibited lower deposition nucleation efficiencies. At −25°C, coated particles exhibited a severe reduction in the degree to which they required water saturation conditions to activate. At −30 and −35°C, these particles nucleated ice in the deposition mode, but the minimum RH_w required to nucleate ice was ~ 90%. In the condensation/immersion freezing mode, independent of temperature, bare and coated particles showed similar ice nucleating behaviors above $RH_w = 105\%$.

XRD analyses were performed to understand why coated particles have reduced efficiency in the deposition mode. The XRD patterns revealed that each dust type consists of several minerals, such as illite, montmorillonite, quartz, calcite, albite, and orthoclase, and is crystalline in nature. After coating, we observed that the peak intensity of these minerals disappeared, indicating that particles became amorphous. This reaction suggests that acid treatment alters the crystallinity and causes structural disorder. Further analysis revealed the evidence for this crystallographic misfit; we found that the crystallographic properties (i.e., lattice parameters and crystallite sizes) of bare and coated particles were different for montmorillonite and K-feldspar minerals. These XRD results indicate that acid treatment causes structural deformations, and the lack of structured order reduced the ice nucleation properties of coated particles in the deposition mode.

We also investigated the sensitivity of the coating apparatus on ice nucleation efficiency. In these experiments, ATD particles were heated in the coating apparatus, and their ice nucleation properties were investigated. We observed that heated and bare particles had similar ice nucleation properties. The XRD patterns also revealed that heated and bare particles had nearly identical peaks. This result confirms that we did not inadvertently modify the physical and chemical properties of the dust particles before their ice nucleation properties were studied. The model results show that reduced ice nucleation efficiency of coated particles decreases the ice number concentration and ice water content significantly. A smaller ice crystal number concentration and ice water content leads to more supercooled liquid droplets in mixed-phase clouds and delays the initiation of precipitation. In addition, fewer IN will consume less water vapor through a heterogeneous ice nucleation process, such that ice supersaturation can build up more easily. Therefore, homogeneous ice nucleation will happen more frequently at temperatures < -38°C.

Appendix A: Coating Thickness Calculations

We estimated the coating thickness by using simple acid molecule condensation parameterization. Assumptions were made as the thermodynamic and flow conditions within coating apparatus were not ideal, and these assumptions affected the coating thickness estimates. Therefore, the thicknesses to which we refer should be only viewed as rough estimates. We have assumed that all acid molecules have condensed to the aerosol particles within a short period of time. The airflow within the apparatus could have been turbulent, so the bulk acid vapor concentration may not be constant. This can vary in space and time. We visually observed acid condensation on the inside surfaces of the apparatus, particularly at the higher temperature (150°C). This effect can reduce the bulk acid vapor concentration. In addition, although we insulated the coating apparatus well enough and the acid bath was maintained at a defined temperature throughout the experiment, we cannot confirm that the temperature distribution within the unit was uniform. Temperature distribution does affect the bulk acid vapor concentration field.

We can estimate the coating thickness using acid condensation rate expression [*Kreidenweis and Seinfeld*, 1988; *Russell et al*., 1994; *Seinfeld and Pandis*, 2006] as follows:

$$R_c = 4\pi r_p D_f f(Kn) D_i (P - P_s),$$

where

R_c = condensation rate of sulfuric acid to a particle of radius, r_p (in m), in molecules/s,
D_f = diffusion coefficient of sulfuric acid molecules in air (set to 1E−5 m^2/s),

$f(Kn)$ = coefficient correction for free molecular effects,

$$f(Kn) = \frac{1 + Kn}{1 + 1.71Kn + 1.33Kn^2}$$

Kn = Knudsen number,

D_i = coefficient correction for the interfacial mass transport,

$$D_i = \left(1 + 1.33Knf(Kn)\left(\frac{1}{a_c} - 1\right)\right)^{-1}$$

a_c = an accommodation coefficient = 0.02

P = bulk vapor concentration of the sulfuric acid in molecules/m^3

$$P = \frac{S_v N_A}{R^* T}$$

S_v = vapor pressure of the sulfuric acid at temperature (T in K),

N_A = Avogadro constant = 6.022E23 molecules/mol,

R^* = Universal gas constant = 8.314 J mol^{-1} K^{-1},

P_s = vapor concentration of sulfuric acid at the particle surface. This was assumed zero for simplicity as we do not know the solubility and activity coefficients of reaction products that formed after acid reaction.

Mass of acid condensed to the particles was calculated using R_c, molar mass of acid (= 0.09808 kg/mol), and N_A quantities. Further, assuming particle and acid density as 1750 kg/m^3 and 1830 kg/m^3, respectively, the coating thickness of ~ 1000 ± 200 particles was calculated. Size of the acid molecules was assumed 0.45 nm.

Acknowledgments

The work was supported by the Office of Science of the U.S. Department of Energy (DOE) as part of the Atmospheric System Research Program. Support for Cassandra Sanders was provided by the U.S. DOE Community College Internship program. We thank Jerome Fast and Elaine King, respectively, for their support of this study. We are grateful for the technical support provided by Danny Nelson. We thank Tamas Varga for performing XRD analysis at Environmental Molecular Sciences Laboratory, which is a national scientific user facility located at Pacific Northwest National Laboratory in Richland, Washington. We also thank three anonymous reviewers for their time and efforts in reviewing this paper. Data supporting sections 2.1, 3.1, 3.2, and 3.4 and Figure 7 are available in the supporting information. This research was performed at the Atmospheric Measurement Laboratory, an atmospheric sciences laboratory at Pacific Northwest National Laboratory (PNNL). PNNL is operated by the U.S. DOE by Battelle Memorial Institute under contract DE-AC05-76RL0 1830.

References

Andreae, M. O., R. J. Charlson, F. Bruynseels, H. Storms, R. Van Grieken, and W. Maenhaut (1986), Internal mixture of sea salt, silicates and excess sulfate in marine aerosols, *Science*, *232*, 1620–1623.

Atkinson, J. D., B. J. Murray, M. T. Woodhouse, T. F. Whale, K. J. Baustian, K. S. Carslaw, S. Dobbie, D. O'Sullivan, and T. L. Malkin (2013), The importance of feldspar for ice nucleation by mineral dust in mixed-phase clouds, *Nature*, *498*(7454), 355–358, doi:10.1038/nature12278.

Baklanov, A. M., B. Gorbunov, N. A. Kakutkina, S. I. Sidorov, N. A. Silin, and S. B. Hvan (1991), The influence of lead iodide aerosol dispersity on its ice-forming activity, *J. Aerosol Sci.*, *22*, 9–14, doi:10.1016/0021-8502(91)90089-Z.

Baron, P. A., and K. Willeke (2001), *Aerosol Measurement: Principles, Techniques, and Applications*, 2nd ed., pp. 61–82, Wiley-Interscience, New York.

Bauer, S. E., M. I. Mishchenko, A. A. Lacis, S. Zhang, J. Perlwitz, and S. M. Metzger (2007), Do sulfate and nitrate coatings on mineral dust have important effects on radiative properties and climate modeling?, *J. Geophys. Res.*, *112*, D06307, doi:10.1029/2005JD006977.

Broadley, S. L., B. J. Murray, R. J. Herbert, J. D. Atkinson, S. Dobbie, T. L. Malkin, E. Condliffe, and L. Neve (2012), Immersion mode heterogeneous ice nucleation by an illite rich powder representative of atmospheric mineral dust, *Atmos. Chem. Phys.*, *12*, 287–307, doi:10.5194/acp-12-287-2012.

Chernoff, D., and A. Bertram (2010), Effects of sulfate coatings on the ice nucleation properties of a biological ice nucleus and several types of minerals, *J. Geophys. Res.*, *115*, D20205, doi:10.1029/2010JD014254.

Connolly, P. J., O. Möhler, P. R. Field, H. Saathoff, R. Burgess, T. Choularton, and M. Gallagher (2009), Studies of heterogeneous freezing by three different desert dust samples, *Atmos. Chem. Phys.*, *9*, 2805–2824, doi:10.5194/acp-9-2805-2009.

Cullity, B. D., and S. R. Stock (2001), *Elements of X-Ray Diffraction*, 3rd ed., Prentice Hall, Upper Saddle River, N. J.

Cziczo, D. J., K. D. Froyd, S. J. Gallavardin, O. Möhler, S. Benz, H. Saathoff, and D. M. Murphy (2009), Deactivation of ice nuclei due to atmospherically relevant surface coating, *Environ. Res. Lett.*, *4*(1–9), 044013, doi:10.1088/1748-9326/4/4/044013.

DeMott, P., K. Sassen, M. Poellot, D. Baumgardner, D. Rogers, S. Brooks, A. Prenni, and S. Kreidenweis (2003), African dust aerosols as atmospheric ice nuclei, *Geophys. Res. Lett.*, *30*(14), 1732, doi:10.1029/2003GL017410.

Eastwood, M. L., S. Cremel, M. Wheeler, B. J. Murray, E. Girard, and A. K. Bertram (2009), Effects of sulfuric acid and ammonium sulfate coatings on the ice nucleation properties of kaolinite particles, *Geophys. Res. Lett.*, *36*, L02811, doi:10.1029/2008GL035997.

Edwards, G. R., and L. F. Evans (1960), Ice nucleation by silver iodide: I. Freezing vs sublimation, *J. Meteor.*, *17*, 627–634.

Ervens, B., and G. Feingold (2012), On the representation of immersion and condensation freezing in cloud models using different nucleation schemes, *Atmos. Chem. Phys.*, *12*, 5807–5826, doi:10.5194/acp-12-5807-2012.

Fairlie, T. D., D. J. Jacob, J. E. Dibb, B. Alexander, M. A. Avery, A. van Donkelaar, and L. Zhang (2010), Impact of mineral dust on nitrate, sulfate, and ozone in transpacific Asian pollution plumes, *Atmos. Chem. Phys.*, *10*, 3999–4012, doi:10.5194/acp-10-3999-2010.

Friedman, B., G. Kulkarni, J. Beránek, A. Zelenyuk, J. A. Thornton, and D. J. Cziczo (2011), Ice nucleation and droplet formation by bare and coated soot particles, *J. Geophys. Res.*, *116*, D17203, doi:10.1029/2011JD015999.

Girard, E., G. Dueymes, P. Du, and A. K. Bertram (2013), Assessment of the effects of acid-coated ice nuclei on the Arctic cloud microstructure, atmospheric dehydration, radiation and temperature during winter, *Int. J. Climatol.*, *33*(3), 599–614, doi:10.1002/joc.3454.

Herich, H., T. Tritscher, A. Wiacek, M. Gysel, E. Weingartner, U. Lohmann, U. Baltensperger, and D. J. Cziczo (2009), Water uptake of clay and desert dust aerosol particles at sub- and supersaturated water vapor conditions, *Phys. Chem. Chem. Phys.*, *11*(36), 7804–7809.

Hoose, C., and O. Möhler (2012), Heterogeneous ice nucleation on atmospheric aerosols: A review of results from laboratory experiments, *Atmos. Chem. Phys.*, *12*, 9817–9854.

Hoose, C., U. Lohmann, R. Erdin, and I. Tegen (2008), Global influence of dust mineralogical composition on heterogeneous ice nucleation in mixed-phase clouds, *Environ. Res. Lett.*, *3*, 025003, doi:10.088/1748-9326/3/2/025003.
Hoose, C., J. E. Kristjánson, J.-P. Chen, and A. Hazra (2010), A classical-theory-based parameterization of heterogeneous ice nucleation by mineral dust, soot, and biological particles in a global climate model, *J. Atmos. Sci.*, *67*, 2483–2503, doi:10.1175/2010JAS3425.1.
Jeong, G. Y. (2008), Bulk and single-particle mineralogy of Asian dust and a comparison with its source soils, *J. Geophys. Res.*, *113*, D02208, doi:10.1029/2007JD008606.
Kanji, Z. A., O. Florea, and J. P. D. Abbatt (2008), Ice formation via deposition nucleation on mineral dust and organics: Dependence of onset relative humidity on total particulate surface area, *Environ. Res. Lett.*, *3*, 025004, doi:10.1088/1748-9326/3/2/025004.
Kanji, Z. A., A. Welti, C. Chou, O. Stetzer, and U. Lohmann (2013), Laboratory studies of immersion and deposition mode ice nucleation of ozone aged mineral dust particles, *Atmos. Chem. Phys. Discuss.*, *13*(4), 8701–8767, doi:10.5194/acpd-13-8701-2013.
Knopf, D. A., and T. Koop (2006), Heterogeneous nucleation of ice on surrogates of mineral dust, *J. Geophys. Res.*, *111*, D12201, doi:10.1029/2005JD006894.
Koehler, K. A., S. M. Kreidenweis, P. J. DeMott, M. D. Petters, A. J. Prenni, and O. Möhler (2010), Laboratory investigations of the impact of mineral dust aerosol on cold cloud formation, *Atmos. Chem. Phys.*, *10*, 11,955–11,968, doi:10.5194/acp-10-11955-2010.
Kojima, T., P. R. Buseck, Y. Iwasaka, A. Matsuki, and D. Trochkine (2006), Sulfate-coated dust particles in the free troposphere over Japan, *Atmos. Res.*, *82*, 698–708.
Koop, T., B. Luo, A. Tsias, and T. Peter (2000), Water Activity as the determinant for homogeneous ice nucleation in aqueous solutions, *Nature*, *406*, 611–614.
Kreidenweis, S., and J. Seinfeld (1988), Nucleation of sulfuric acid–water and methanesulfonic acid–water solution particles: Implications for the atmospheric chemistry of organo-sulfur species, *Atmos. Environ.*, *22*(2), 283–296.
Kulkarni, G., and S. Dobbie (2010), Ice nucleation properties of mineral dust particles: Determination of onset RH, IN active fraction, nucleation time-lag, and the effect of active sites on contact angles, *Atmos. Chem. Phys.*, *10*, 95–105, doi:10.5194/acp-10-95-2010.
Kulkarni, G., S. Dobbie, and J. B. McQuaid (2009), A new thermal gradient ice nucleation diffusion chamber instrument: Design, development and first results using Saharan mineral dust, *Atmos. Meas. Tech.*, *2*, 221–229, doi:10.5194/amt-2-221-2009.
Kulkarni, G., J. Fan, J. M. Comstock, X. Liu, and M. Ovchinnikov (2012), Laboratory measurements and model sensitivity studies of dust deposition ice nucleation, *Atmos. Chem. Phys.*, *12*, 7295–7308, doi:10.5194/acp-12-7295-2012.
Levin, Z., E. Ganor, and V. Gladstein (1996), The effects of desert particles coated with sulfate on rain formation in the eastern Mediterranean, *J. Appl. Meteorol.*, *35*, 1511–1523.
Liu, X., and J. E. Penner (2005), Ice nucleation parameterization for global models, *Meteorol. Z.*, *14*, 499–514.
Liu, X., J. E. Penner, and M. Herzog (2005), Global modeling of aerosol dynamics: Model description, evaluation, and interactions between sulfate and nonsulfate aerosols, *J. Geophys. Res.*, *110*, D18206, doi:10.1029/2004JD005674.
Liu, X., et al. (2012a), Toward a minimal representation of aerosols in climate models: Description and evaluation in the Community Atmosphere Model CAM5, *Geosci. Model Dev.*, *5*, 709–739, doi:10.5194/gmd-5-709-2012.
Liu, X., X. Shi, K. Zhang, E. Jensen, A. Gettelman, D. Barahona, A. Nenes, and P. Lawson (2012b), Sensitivity studies of dust ice nuclei effect on cirrus clouds with the Community Atmosphere Model CAM5, *Atmos. Chem. Phys.*, *12*, 12,061–12,079, doi:10.5194/acp-12-12061-2012.
Liu, X., Y. Wang, S. Ghan, N. Mahowald, and R. Scanza (2013), Simulations of global impact of dust speciation on mixed-phase clouds through ice nucleation, Paper presented at 93rd AMS Annual Meeting, *Am. Meteorol. Soc.*, Austin, Tex.
Luria, M., and H. Sievering (1991), Heterogeneous and homogeneous oxidation of SO_2 in the remote marine atmosphere, *Atmos. Environ.*, *25A*, 1489–1496.
Makó, É., Z. Senkár, J. Kristóf, and V. Vágvölgyi (2006), Surface modification of mechanochemically activated kaolinites by selective leaching, *J. Colloid Interface Sci.*, *294*(2), 362–370.
Mamane, Y., and K. E. Noll (1985), Characterization of large particles at a rural site in the eastern United States: Mass distribution and individual particle analysis, *Atmos. Environ.*, *19*, 611–622.
Marcolli, C. (2014), Deposition nucleation viewed as homogeneous or immersion freezing in pores and cavities, *Atmos. Chem. Phys.*, *14*, 2071–2104, doi:10.5194/acp-14-2071-2014.
Marcolli, C., S. Gedamke, T. Peter, and B. Zobrist (2007), Efficiency of immersion mode ice nucleation on surrogates of mineral dust, *Atmos. Chem. Phys.*, *7*, 5081–5091.
Melo, J. D. D., T. Costa, A. Medeiros, and C. A. Paskocimas (2010), Effects of thermal and chemical treatments on physical properties of kaolinite, *Ceram. Int.*, *36*, 33–38.
Möhler, O., S. Benz, H. Saathoff, M. Schnaiter, R. Wagner, J. Schneider, S. Walter, V. Ebert, and S. Wagner (2008), The effect of organic coating on the heterogeneous ice nucleation efficiency of mineral dust aerosols, *Environ. Res. Lett.*, *3*(2), 025007, doi:10.1088/1748-9326/3/2/025007.
Murphy, D. M., and T. Koop (2005), Review of the vapour pressures of ice and supercooled water for atmospheric applications, *Q. J. R. Meteorol. Soc.*, *131*, 1539–1565.
Murray, B. J., D. O'Sullivan, J. D. Atkinson, and M. E. Webb (2012), Ice nucleation by particles immersed in supercooled cloud droplets, *Chem. Soc. Rev.*, *41*, 6519–6554, doi:10.1039/c2cs35200a.
Neale, R. B., et al. (2010), Description of the NCAR Community Atmosphere Model (CAM5.0), *Tech. Rep. NCAR/TN-486-STR*, NCAR. [Available at http://www.cesm.ucar.edu/models/cesm1.0/cam/] (last access: 8 January 2013).]
Niedermeier, D., et al. (2010), Heterogeneous freezing of droplets with immersed mineral dust particles—Measurements and parameterization, *Atmos. Chem. Phys.*, *10*(8), 3601–3614, doi:10.5194/acp-10-3601-2010.
Niedermeier, D., et al. (2011), Experimental study of the role of physicochemical surface processing on the IN ability of mineral dust particles, *Atmos. Chem. Phys.*, *11*(21), 11,131–11,144, doi:10.5194/acp-11-11131-2011.
Niemand, M., et al. (2012), A particle-surface-area-based parameterization of immersion freezing on desert dust particles, *J. Atmos. Sci.*, *69*, 3077–3092, doi:10.1175/jasd-11–0249.1.
Panda, A. K., B. G. Mishra, D. K. Mishra, and R. K. Singh (2010), Effect of sulphuric acid treatment on the physico-chemical characteristics of kaolin clay, *Colloids Surf., A*, *363*, 98–104, doi:10.1016/j.colsurfa.2010.04.022.
Prospero, J. M., R. T. Nees, and M. Uematsu (1987), Deposition rate of particulate and dissolved aluminum derived from Saharan dust in precipitation at Miami, Florida, *J. Geophys. Res.*, *92*(D12), 14,723–14,731, doi:10.1029/JD092iD12p14723.
Pruppacher, R. H., and J. D. Klett (1997), *Microphysics of Clouds and Precipitation*, pp. 326–341, Kluwer Acad, Dordrecht, Netherlands.
Rajesh, N., B. G. Mishra, and P. K. Pareek (2008), Solid phase extraction of chromium(VI) from aqueous solutions by adsorption of its diphenylcarbazide complex on a mixed bed adsorbent (acid activated montmorillonite-silica gel) column, *Spectrochim. Acta, Part A*, *69*, 612–618.
Reitz, P., et al. (2011), Surface modification of mineral dust particles by sulphuric acid processing: Implications for ice nucleation abilities, *Atmos. Chem. Phys.*, *11*, 7839–7858, doi:10.5194/acp-11-7839-2011.

Rogers, D. C. (1988), Development of a continuous flow thermal gradient diffusion chamber for ice nucleation studies, *Atmos. Res.*, *22*, 149–181.

Russell, L. M., S. N. Pandis, and J. H. Seinfeld (1994), Aerosol production and growth in the marine boundary layer, *J. Geophys. Res.*, *99*, 20,989–21,003, doi:10.1029/94JD01932.

Seinfeld, J. H., and S. N. Pandis (2006), *Atmospheric Chemistry and Physics: From Air Pollution to Climate Change*, 2nd ed., Wiley, New York.

Shi, Z., D. Zhang, M. Hayashi, H. Ogata, H. Ji, and W. Fujiie (2008), Influences of sulfate and nitrate on the hygroscopic behaviour of coarse dust particles, *Atmos. Environ.*, *42*(4), 822–827, doi:10.1016/j.atmosenv.2007.10.037.

Stetzer, O., B. Baschek, F. Luond, and U. Lohmann (2008), The Zurich Ice Nucleation Chamber (ZINC)—A new instrument to investigate atmospheric ice formation, *Aerosol Sci. Technol.*, *42*, 64–74.

Stumm, W. (1992), *Chemistry of the Solid-Water Interface*, Willey-Interscience, New York.

Sullivan, R. C., S. A. Guazzotti, D. A. Sodeman, and K. A. Prather (2007), Direct observations of the atmospheric processing of Asian mineral dust, *Atmos. Chem. Phys.*, *7*, 1213–1226.

Sullivan, R. C., et al. (2010a), Irreversible loss of ice nucleation active sites in mineral dust particles caused by sulphuric acid condensation, *Atmos. Chem. Phys.*, *10*, 11,471–11,487, doi:10.5194/acp-10-11471-2010.

Sullivan, R. C., M. J. K. Moore, M. D. Petters, S. M. Kreidenweis, O. Qafoku, A. Laskin, G. C. Roberts, and K. A. Prather (2010b), Impact of particle generation method on the apparent hygroscopicity of insoluble mineral particles, *Aerosol Sci. Technol.*, *44*, 830–846, doi:10.1080/02786826.2010.497514.

Sullivan, R. C., L. Miñambres, P. J. DeMott, A. J. Prenni, C. M. Carrico, E. J. Levin, and S. M. Kreidenweis (2010c), Chemical processing does not always impair heterogeneous ice nucleation of mineral dust particles, *Geophys. Res. Lett.*, *37*, L24805, doi:10.1029/2010GL045540.

Tobo, Y., P. J. DeMott, M. Raddatz, D. Niedermeier, S. Hartmann, S. M. Kreidenweis, F. Stratmann, and H. Wex (2012), Impacts of chemical reactivity on ice nucleation of kaolinite particles: A case study of levoglucosan and sulfuric acid, *Geophys. Res. Lett.*, *39*, L19803, doi:10.1029/2012GL053007.

Volzone, C., and J. Ortiga (2006), Removal of gases by thermal-acid leached kaolinitic clays: Influence of mineralogical composition, *Appl. Clay Sci.*, *32*, 87–93.

Volzone, C., and J. Ortiga (2011), SO_2 gas adsorption by modified kaolin clays: Influence of previous heating and time acid treatments, *J. Environ. Manage.*, *92*, 2590–2595, doi:10.1016/j.jenvman.2011.05.031.

Volzone, C., O. Masini, N. A. Comelli, L. M. Grzona, E. N. Ponzi, and M. I. Ponzi (2005), α-Pinene conversion by modified-kaolinitic clay, *Mater. Chem. Phys.*, *93*, 296–300.

Vonnegut, B. (1947), The nucleation of ice formation by silver iodide, *J. Appl. Phys.*, *18*, 593, doi:10.1063/1.1697813.

Warren, B. E. (1990), *X-Ray Diffraction*, Dover, Mineola, New York.

Welti, A., F. Lüönd, O. Stetzer, and U. Lohmann (2009), Influence of particle size on the ice nucleating ability of mineral dusts, *Atmos. Chem. Phys.*, *9*, 6705–6715.

Wex, H., P. DeMott, Y. Tobo, S. Hartmann, M. Raddatz, T. Clauss, D. Niedermeier, and F. Stratmann (2013), Kaolinite particles as ice nuclei: Learning from the use of different types of kaolinite and different coatings, *Atmos. Chem. Phys. Disc.*, *13*, 30,311–30,348.

Wheeler, M. J., and A. K. Bertram (2012), Deposition nucleation on mineral dust particles: A case against classical nucleation theory with the assumption of a single contact angle, *Atmos. Chem. Phys.*, *12*, 1189–1201, doi:10.5194/acp-12-1189-2012.

Yakobi-Hancock, J. D., L. A. Ladino, and J. P. D. Abbatt (2013), Feldspar minerals as efficient deposition ice nuclei, *Atmos. Chem. Phys.*, *13*(22), 11,175–11,185, doi:10.5194/acp-13-11175-2013.

Yang, Z., A. K. Bertram, and K. C. Chou (2011), Why do sulfuric acid coatings influence the ice nucleation properties of mineral dust particles in the atmosphere?, *J. Phys. Chem. Lett.*, *2*, 1232–1236, doi:10.1021/jz2003342.

Zhang, K., X. Liu, M. Wang, J. Comstock, D. Mitchell, S. Mishra, and G. Mace (2013), Evaluating and constraining ice cloud parameterizations in CAM5 using aircraft measurements from the SPARTICUS campaign, *Atmos. Chem. Phys.*, *13*, 4963–4982, doi:10.5194/acp-13-4963-2013.

Zhang, M. H., and J. L. Lin (1997), Constrained variational analysis of sounding data based on column-integrated budgets of mass, heat, moisture, and momentum: Approach and application to ARM measurements, *J. Atmos. Sci.*, *54*, 1503–1524.

Zhang, M. H., J. L. Lin, R. T. Cederwall, J. J. Yio, and S. C. Xie (2001), Objective analysis of ARM IOP data: Method and sensitivity, *Mon. Weather Rev.*, *129*, 295–311.

Zhao, H., C. H. Zhou, L. M. Wu, J. Y. Lou, N. Li, H. M. Yang, D. S. Tong, and W. H. Yu (2013), Catalytic dehydration of glycerol to acrolein over sulfuric acid-activated montmorillonite catalysts, *Appl. Clay Sci.*, *74*, 154–162.

Zobrist, B., C. Marcolli, T. Peter, and T. Koop (2008), Heterogeneous ice nucleation in aqueous solutions: The role of water activity, *J. Phys. Chem. A*, *112*, 3965–3975.

Zuberi, B., A. K. Bertram, C. A. Cassa, L. T. Molina, and M. J. Molina (2002), Heterogeneous nucleation of ice in $(NH_4)_2SO_4$-H_2O particles with mineral dust immersions, *Geophys. Res. Lett.*, *29*(10), 1504, doi:10.1029/2001GL014289.